Received: 8 May 2020 | Revised: 12 August 2020 | Accepted: 2 September 2020

DOI: 10.1002/eom2.12056

REVIEW

EcoMat FUNCTIONAL MATERIALS FOR GREEN ENERGY AND ENVIRONMENT WILEY

Practical energy densities, cost, and technical challenges for magnesium-sulfur batteries

Rameez Razaq[1,2] | **Ping Li**[2] | **Yulong Dong**[2] | **Yao Li**[1,3] | **Ya Mao**[4] | **Shou-Hang Bo**[2]

[1]State Key Laboratory of Metal Matrix Composites, Shanghai Jiao Tong University, Shanghai, China

[2]University of Michigan - Shanghai Jiao Tong University Joint Institute, Shanghai Jiao Tong University, Shanghai, China

[3]Department of Nuclear Science and Engineering, Massachusetts Institute of Technology, Cambridge, Massachusetts

[4]State Key Laboratory of Space Power-Sources Technology, Shanghai Institute of Space Power-Sources, Shanghai, China

Correspondence
Yao Li, State Key Laboratory of Metal Matrix Composites, Shanghai Jiao Tong University, 800 Dong Chuan Road, Minhang District, Shanghai 200240, China.
Email: liyaosjtu@sjtu.edu.cn

Ya Mao, State Key Laboratory of Space Power-Sources Technology, Shanghai Institute of Space Power-Sources, 2965 Dong Chuan Road, Minhang District, Shanghai 200240, China.
Email: maoya0106@163.com

Shou-Hang Bo, University of Michigan - Shanghai Jiao Tong University Joint Institute, Shanghai Jiao Tong University 800 Dong Chuan Road, Minhang District, Shanghai 200240, China.
Email: shouhang.bo@sjtu.edu.cn

Funding information
China Scholarship Council; National Natural Science Foundation of China, Grant/Award Number: 51801121; Oceanic Interdisciplinary Program of Shanghai Jiao Tong University, Grant/Award Number: SL2020MS025; Shanghai Commission of Science and Technology, Grant/Award Number: 18ZR1421000

Abstract

Amid burgeoning environmental concerns, electrochemical energy storage has rapidly gained momentum. Among the contenders in the "beyond lithium" energy storage arena, the magnesium-sulfur (Mg/S) battery has emerged as particularly promising, owing to its high theoretical energy density. However, the gap between fundamental research and practical application is still hindering the commercialization of Mg/S batteries. Here, through reviewing the recent developments of Mg/S batteries technologies, especially with respect to energy density and cost, we present the primary technical challenges on both materials and device level to surpass the energy density and cost-effectiveness of lithium-ion battery. While the high electrolyte-sulfur ratio and the expensive liquid electrolyte are significantly limiting the practical application of Mg/S batteries, we found that solid-state Mg electrolyte appears to be a feasible solution on the basis of energy density and cost evaluation.

KEYWORDS

cost analysis, magnesium-sulfur battery, practical energy density, solid-state electrolytes

Rameez Razaq and Ping Li should be considered joint first author.

1 | INTRODUCTION

The ever-increasing quest for battery technologies with long life, high energy density, materials sustainability and safety, has led to the development of advanced energy-storage systems. In the field of rechargeable batteries, Lithium-ion batteries (LIBs) have dominated the numerous application fields such as portable electronics, electric vehicles, grid, and residential energy storage.[1] However, after more than three decades of development, the current LIBs technology is impending a fundamental limit in terms of energy density, safety, and cost.[2,3] For electric vehicle applications, there is still an urgent demand to further upgrade the energy density to improve the driving range to at least 500 km.[4] Hence, there is tremendous effort to develop battery technologies that could offer high energy density. On the one hand, Li metal-based batteries, such as all-solid-state batteries[5] are extensively considered to surpass LIBs in terms of specific gravimetric (*Eg*) (Wh kg^{-1}) and volumetric energy density (*Ev*) (Wh L^{-1}). On the other hand, the cathode active materials of LIBs are usually based on critical elements, especially cobalt (Co) and nickel (Ni), which increases the cost of LIBs and imposes potential supply-chain risk.[6] Alternatively, metal-air batteries such as Fe-O_2, Zn-O_2, Mg-O_2, and Li-O_2 have been widely studied due to high theoretical specific energy density (764, 1084, 2859, and 3505 Wh kg^{-1}, respectively) for emerging application such as electric vehicles and grids storage.[7-13] However, for these emerging energy storage systems, it remains challenging to attain practical energy density comparable with LIBs. Therefore, other battery systems, such as Na/S batteries,[14] and magnesium-sulfur (Mg/S) batteries,[15] have been increasingly investigated.

In view of the cost of LIBs, the rapid expansion of Li-ion technology in various applications has led to the increasing price of critical elements, such as Li and Co.[6] Furthermore, the commercialization of Li metal-based all-solid-state batteries could be accompanied with an increase in cost, due to the high cost of Li-metal ingot (50-130 \$ kg^{-1}) and the solid electrolyte.[16] Moreover, the processing and handling of the highly reactive thin film Li metal give rise to additional process cost, while material cost for solid electrolytes would need to compete with relatively low-cost liquid electrolytes for LIBs.[16] Since the raw material cost for S is very low (0.22 \$ kg^{-1}),[17] cost for Li/S batteries in a very optimistic scenario could be around 100 \$ kWh at the cell level[18] making them a low-cost alternative to LIBs in certain markets.[16,19,20] In Mg/S batteries, the costly Li metal would be replaced by cheaper Mg metal (4.0 \$ kg^{-1}).[21] A potentially lower material price for Mg/S batteries than that of Li/S batteries can be achieved.

This driving force of cost reduction inspired the application of earth-abundant Mg metal as an anode and S as a cathode material in Mg/S batteries.[22] Considering the high density (1.738 g cm^{-3}) and the divalent nature of Mg^{2+}, Mg metal possesses a higher theoretical volumetric capacity of 3832 mAh cm^{-3} than Li (2062 mAh cm^{-3}).[23] In addition, Mg has a reduction potential of −2.4 V vs SHE, and it can be handled in air. As Mg has a much lower tendency to form dendrites and the melting point (650°C) is substantially higher than that for Li (181°C), it is considered a safer and more reliable anode material.[24]

A typical Mg/S battery is comprised of an S-carbon-based composite cathode, an organic electrolyte, and an Mg metal anode.[22] The Mg metal is oxidized to produce Mg^{2+} which migrates to the S cathode through the organic electrolyte and separator, while electrons arrive at the active S material via an external electrical circuit.[25-28]

$$\text{Anode}: Mg^0 \leftrightarrow Mg^{2+} + 2e^-$$

$$\text{Cathode}: S_8 + 8Mg^{2+} + 16e^- \leftrightarrow MgS$$

Assuming 1672 mAh g^{-1} cathode capacity and a mean discharge voltage of 1.77 V, these reactions deliver high theoretical gravimetric and volumetric energy density of 1684 Wh kg^{-1} and 3221 Wh L^{-1}, respectively. The theoretical volumetric energy density of Mg/S batteries exceeds that (2856 Wh L^{-1}) of Li/S batteries. However, the theoretical gravimetric energy density of Mg/S batteries is lower than that (2600 Wh kg^{-1}) of Li/S batteries.[26-31]

Regardless of the high energy density, cost-effectiveness, and safety, several key challenges still need to be addressed to realize the commercialization of Mg/S batteries, which we briefly summarize as follows:

1. A suitable electrolyte that should be chemically compatible with the electrophilic S and capable of reversible Mg deposition/dissolution.[32,33]
2. Polysulfide shuttle due to dissolution of intermediates Mg-PS_x into the electrolyte.[26,34]
3. The rapid capacity decay caused by the dissolution and migration of Mg-PS_x species during cycling.[19,28,35]
4. The low utilization of S due to low electrical conductivity of S and resultant MgS.[35,36]
5. The formation of Mg dendrites at high current densities.[24,37-41]
6. The sluggish Mg^{2+} transport; The Mg^{2+} migration barrier calculated for MgS is ∼900 meV, suggesting that MgS can be electrochemically inactive and can significantly limit Mg transport in the composite electrode.[42,43]

7. The experimentally observed low discharge potential (around 1.1 V or below).[26,44]
8. Formation of solid electrolyte interphase (SEI) and inactive MgO passivating film on Mg surface when exposed to air that is impermeable to Mg^{2+}.[23,45,46] For an extensive review of these challenges and proposed solutions, we refer the readers to previously published reviews.[22,23,32,47,48] We further note that many similar challenges also exist in Li/S and Na/S systems, such as low S loading, high electrolyte to S ratio (E/S), insulating nature of S, polysulfides shuttle, and dendritic growth of metal anode.[19,49]

Considerable efforts have been made to improve the electrochemical performance of Mg/S batteries which have been summarized in a number of reviews.[22,23,47,48,50] However, a critical analysis on the practical energy densities, cost, and technical challenges for Mg/S batteries is still lacking. In this review, we first summarize the current status of Mg/S batteries in view of materials development and literature review analysis. In the second section, we systematically investigate the relationships between the energy density, cost, and other parameters of Mg/S cells. Finally, conclusions and future perspectives of high energy density Mg/S batteries are provided.

2 | CURRENT STATUS

2.1 | Material development

Conversion-type S-cathode in Mg/S batteries involve the discharge/charge processes by the reduction and oxidation of elemental S.[15] Various forms of carbon as a conductive matrix (Table S1), such as S-carbon composite ink,[26] active carbon cloth,[51] mesoporous carbon,[28] microporous carbon,[52] CMK-3,[28,53] 2-D GO,[27] graphdiyne,[52] S-/nitrogen-doped carbon,[54] and metal-organic frameworks,[55] have been reported to enhance the utilization of active S. However, the fast capacity decay by these cathode materials was assigned to the shuttle effect caused by soluble polysulfides and severe overcharging in Mg/S system.

Similar to the well-established Li/S and Na/S batteries, carbon is the most frequently used candidate to host S for Mg/S batteries.[56-59] Nonetheless, the physical confinement of polar polysulfides on nonpolar carbon is not enough to reduce the shuttle effect. Henceforth, an improved redox kinetics of S cathode could be realized by applying various electrocatalysts[60-65] that not only chemically trap the S species but also enhance conversion efficiency.

Electrolyte is one of the most important components of the cell and medium for the transfer of Mg ions between the S cathode and the Mg anode in Mg/S batteries during the battery operation.[66-70] Much efforts have been given to design the appropriate electrolytes for Mg/S batteries. It is worth mentioning that the conventional nucleophilic electrolytes are incompatible with electrophilic S causing cell failure.[26,23,52,32] This innovative research on nucleophilic electrolytes was further elaborated on the preparation of nonnucleophilic electrolytes.[28,66,71-76] Apart from the single magnesium salt for electrolytes, dual-salt Mg^{2+}/Li^{+} electrolyte results in smoother Mg plating than that of Mg electrolyte only.[77,78]

Research progress on the development of suitable liquid electrolyte systems for Mg/S batteries is still ongoing (Table S1). The development of novel liquid electrolytes compatible with S cathode clearly depends on utilization of noncorrosive magnesium salts, various solvents, and additives.

Solid-state batteries are promising candidates for overcoming the intrinsic problem associated with liquid electrolyte.[79-81] At present, one of the key challenges in obtaining a suitable solid-state magnesium-based electrolyte lies in the ionic conductivity at room temperature (around 1 $mS\,cm^{-1}$).[79] However, with few exceptions,[82-84] the low room-temperature ionic conductivities are the upmost challenge hampering the application of solid-state electrolytes (SSEs). Henceforth, the development of an appropriate SSE is highly desired for Mg/S batteries.

The energy density of current LIBs can be exceeded when Mg metal anodes are employed.[23,45,85] Currently, different forms of commercial magnesium (99.9% purity or higher) such as foils,[86] discs,[36,87] and plates[45,88,89] are being used to develop Mg/S batteries (Table S1).[90-92]

Apart from different forms of Mg anode, powder-based magnesium anode demonstrated the effectiveness of structure design on the improvement of Mg/S batteries.[93] Similarly Mg_3Bi_2 as an alternative anode material exhibits excellent electrochemical performance.[94] Other than alloys as an anode, polymer electrolytes,[95] protective layer,[96-99] Mg compounds,[42] and magnesium-aluminum-chloride-based electrolytes[100,101] might be effective approaches to protect the Mg metal surface in Mg/S batteries.[97]

Besides designing efficient cathode materials and appropriate electrolytes, modifying the separators also signifies a viable route to trap the Mg-PS_x. Recently, CNF-[25] and TiS_2-[102] coated glass fiber by a vacuum-filtration process were employed as a modified separator. However, the coated separator with the carbon S composite as cathode will decrease the energy density by increasing the thickness of the cell.

2.2 | Literature review analysis

Despite the development in materials, the practical application of high energy density Mg/S batteries is still challenging. Herein, we investigate the materials and parameters of Mg/S batteries from 42 publications between 2011 and 2020 and discuss how these parameters are related to the energy density. All the relevant publications, the reported cell parameters and cycling performance are tabulated in Table S1, Supporting Information.

1. Starting from the cell type, currently used cell for Mg/S batteries are coin cell, Swagelok cell and pouch cell. Then, 67% of them are coin cells, while only 3% used the pouch cell (Figure 1A) due to ease of fabrication with less active material and electrolyte. However, it should be noted that insights obtained from coin cells may not be directly applicable to large pouch cells used in practical applications.
2. From the literature review analysis, 42% published works use the Mg foil as an anode (Figure 1B). However, the electrochemical performance of anodes based on the pressed powder of Mg/C (14%) showed better coulombic efficiencies than those based on an Mg foil.
3. Currently used separators in Mg/S batteries are mainly based on commercial glass fiber, Celgard, and polymer membranes (Figure 1c). From the literature review analysis, generally glass fiber separators (68%) outperform others in terms of thermal stability, porosity, permeability, and ionic conductivity; but they are more costly and require more electrolyte.[78,79]
4. The S content reflects the total S in the whole cathode as wt% S (Figure 1D) which allows the estimation of the capacity of the cell. 50% of publications present the S cathodes with ≤50 wt% S contents, but only 11% of publications report the S cathodes with high S content of over 70 wt%. In other words, constructing high

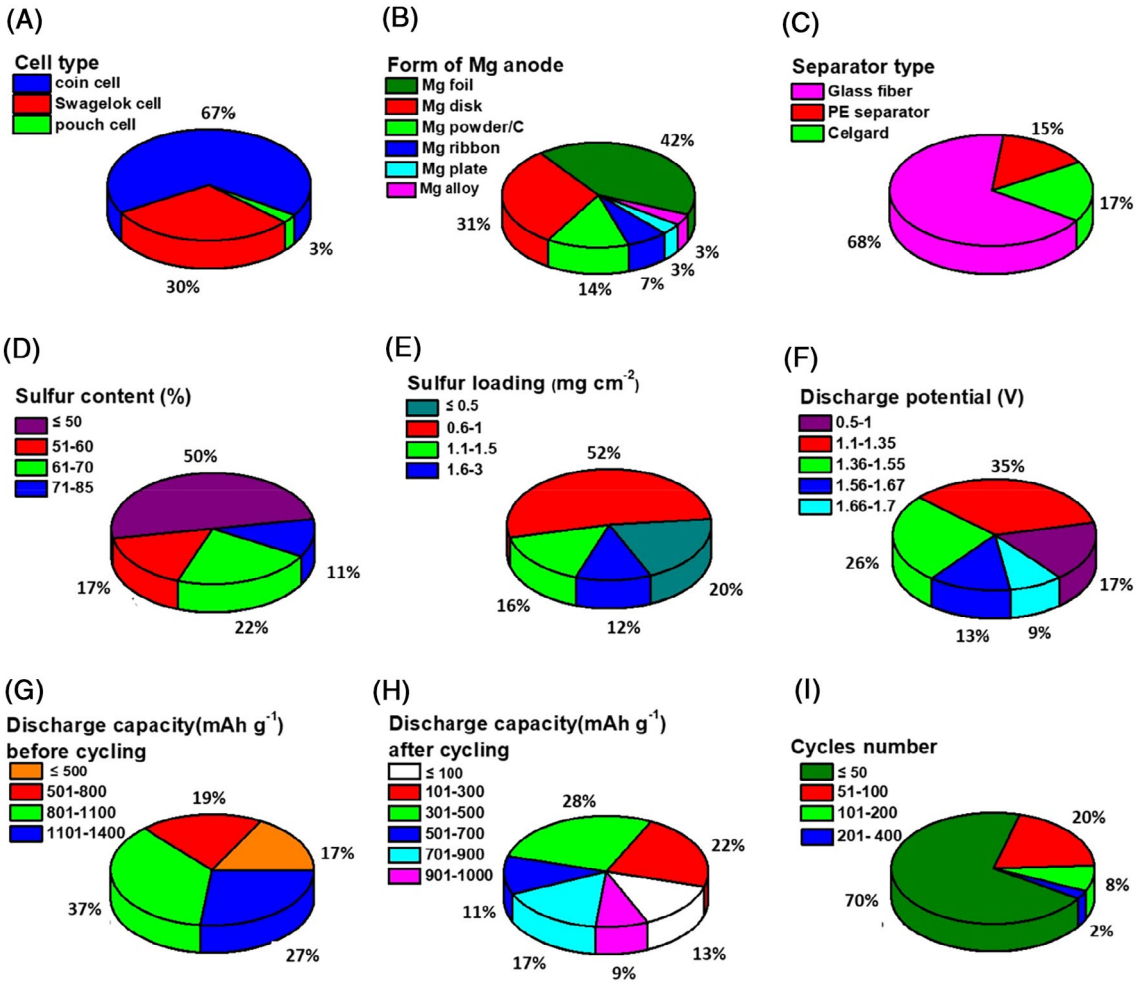

FIGURE 1 Comparative analysis of the materials and parameters of magnesium-sulfur (Mg/S) batteries from 42 publications between 2011 and 2020: A, cell type; B, different forms of Mg anode; C, separator type; D, sulfur contents (wt%); E, sulfur loading (mg cm^{-2}); F, initial discharge potential; G, discharge capacity before cycling; H, discharge capacity after cycling; and I, cycle number

S loading electrodes with S contents higher than 70 wt % is still a challenge due to the extremely low electronic conductivity of S. However, high S content of over 70 wt% in the cathode is necessary to build Mg/S batteries with a high energy density.

5. The areal loading of S is a key parameter for the energy density of practical Mg/S batteries. We summarized the literatures from Table S1 with different S loadings. Most of the publications (52%) have developed S loading cathodes with merely 0.6 to 1 mg cm^{-2} (Figure 1E). To pave the way to practically viable Mg/S batteries, high areal loading of S is essential.
6. Figure 1F shows the literature review analysis of the observed discharge voltages. Nearly 52% of reports present the first discharge voltage potential smaller than 1.35 V; however, only 9% studies showed that discharge potential is close to theoretical potential (1.77 V) meaning that the overpotential in the electrochemical reaction is a significant problem.
7. Most of the studies did not provide any information about the electrolyte volume to S mass (E/S) ratio. Only a few papers reported E/S ratios, which were around 80 to 100 μL mg^{-1} indicating that the E/S ratio has not received enough attention despite its significance.
8. Compared with the S content, the situation of discharge capacity and cycling life are even worse. Although 64% of the electrodes could deliver initial discharge capacities >800 mAh g^{-1} (Figure 1G), the fraction of publications with discharge capacities remaining above 900 mAh g^{-1} after cycling is only 9%, and 63% of them are ≤500 mAh g^{-1} indicating the poor cycling stability (Figure 1H). Moreover, only 2% of them achieved over 201 to 400 cycles (Figure 1I), which cannot meet the requirements for electric vehicles and has much lower cycle life than current LIBs.

When taking these results into consideration, the development of high S loading electrodes with high capacity output and discharge voltage close to the theoretical value, and stabilized cycling performance under low E/S ratio will be the main research direction in the future.

3 | EVALUATION AND TARGET OF HIGH ENERGY DENSITY Mg/S BATTERIES

3.1 | Parameterization of Mg/S batteries components based on gravimetric and volumetric energy density

To illustrate the foundation of energy density evaluation, we first analyze the theoretical *Eg* and *Ev* only considering magnesium anode and S cathode and then move on to practical cells. The theoretical *Eg* and *Ev* can be calculated by Formulas (1) and (2), respectively, with respect to a full-cell electrochemical reaction of Mg + S → MgS:

$$E_g = \frac{2EF}{\sum M} \tag{1}$$

$$E_v = \frac{2EF}{\sum V} \tag{2}$$

where E is the thermodynamic equilibrium voltage, F is the Faraday constant, $\sum M$ and $\sum V$ are the sum of the molar mass and corresponding sum of volume of reactants, respectively.[103] When only Mg and S are considered, $\sum M$ and $\sum V$ are the sum of molar mass and molar volume for Mg and S (ie, 56.37 g mol^{-1} and 27.57 mL mol^{-1}), respectively. The thermodynamic equilibrium voltage at standard state (at the temperature of 298.15 K and the pressure of 1 atm) (E^0) can be calculated by Formulas (3) and (4)

$$\Delta G_r^0 = -2E^0\mathrm{F} \tag{3}$$

$$\Delta G_r^0 = \Delta_f G_{MgS}^0 - \Delta_f G_{Mg}^0 - \Delta_f G_S^0 \tag{4}$$

where ΔG_r^0 is the standard molar Gibbs energy of reaction Mg + S → MgS, $\Delta_f G_{MgS}^0$, $\Delta_f G_{Mg}^0$, and $\Delta_f G_S^0$ are the standard molar Gibbs energy of formation of MgS, Mg, and S, respectively. On the basis of tabulated thermodynamic data,[104] the E^0 is calculated to be 1.77 V at standard state. Combining with Formulas (1) and (2), the theoretical *Eg* and *Ev* are 1684 Wh kg^{-1} and 3221 Wh L^{-1} at standard state, respectively.

Cell-level practical energy density should be considered based on all cell components. Energy density of Mg/S batteries comprising liquid electrolyte is calculated based on a pouch cell. The designed pouch cell is shown in Figure 2A, with a cross-sectional area of 12 × 8 cm^2. Because the liquid electrolyte is facile to flow and leak, we only considered one layer of cathode and one layer of anode instead of multilayered form. However, we note the energy density generally increases in pouch cell when multiple layers of cathode and anode are used. The magnesium foil acts as both anode and anode current collector (an additional current collector may be required if welding the Ni tab with Mg metal is problematic), the thickness of which is designed based on the negative/positive (N/P) capacity ratio of 1.2 with 20% excess Mg stock. N/P capacity ratio of 1:1 on Li metal batteries with artificial SEI has been recently reported by Wang group.[105]

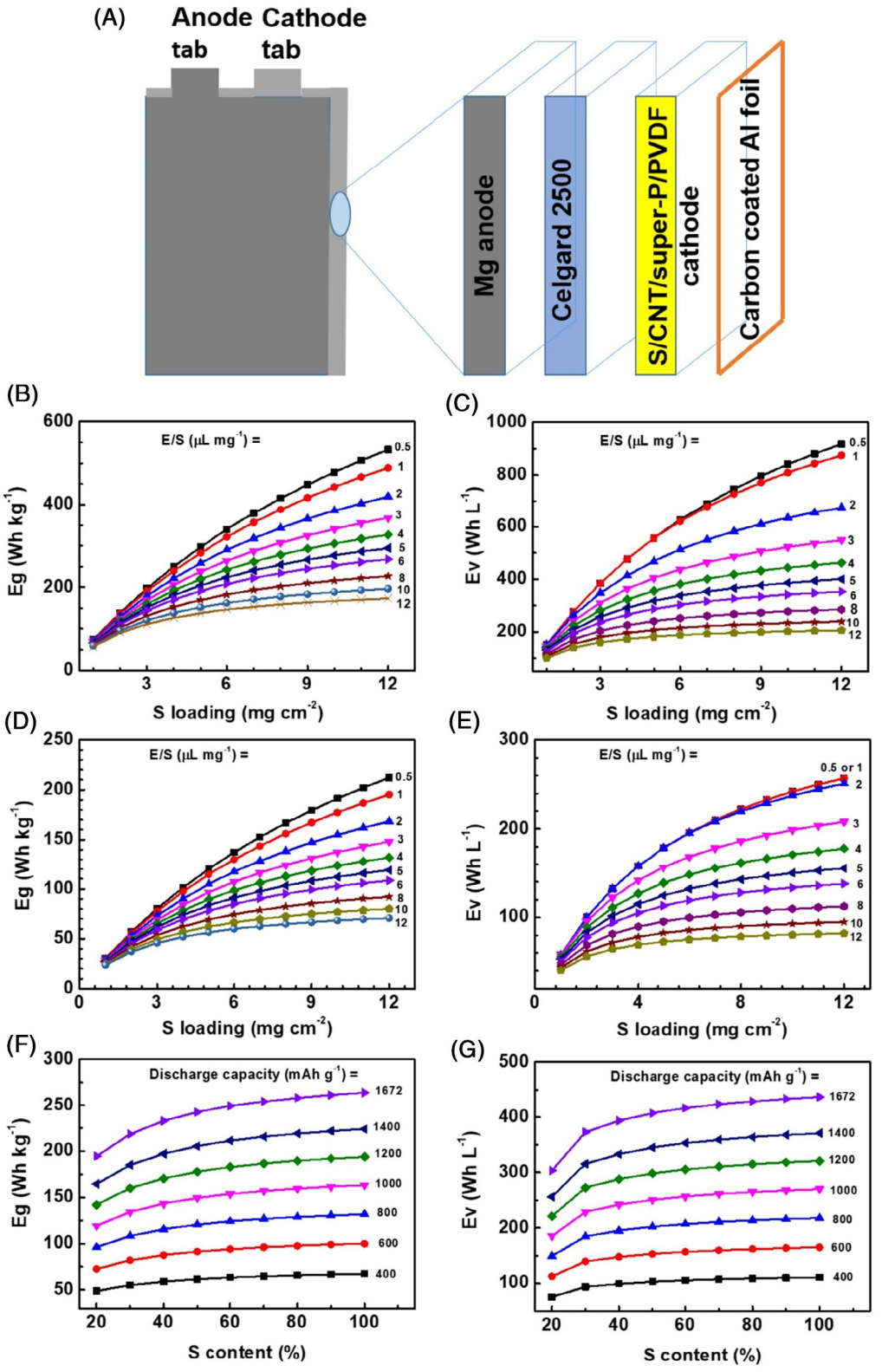

FIGURE 2 Gravimetric and volumetric energy density estimation of magnesium-sulfur (Mg/S) batteries with liquid electrolytes: A, the structure of Mg/S pouch cell with liquid electrolytes; B, the gravimetric; and C, volumetric energy density of ideal cell with 100 wt% sulfur content, 100% sulfur utilization and theoretical discharge voltage of 1.77 V; D, the gravimetric; and E, volumetric energy density of realistic pouch cell with 64 wt% sulfur content, 60.8% sulfur utilization and average discharge voltage of 1.2 V; F, the gravimetric and G, volumetric energy density of pouch cell with fixed sulfur loading of 6 mg cm^{-2}, E/S of 3 μL mg^{-1}, and average discharge voltage of 1.77 V

Considering that Mg metal is less electrochemically active than Li metal, we believe that an N/P ratio of 1.2 is plausible. In this designed Mg/S cell, the liquid electrolyte is chosen as 0.5 M organic magnesium borated-based electrolyte (OMBB) reported by Du et al.[36] The reported liquid electrolytes on Mg/S batteries with more than 50 cycles are summarized in Excel S1 (SI). The energy densities after cycles in Excel S1 are ranked, which is the product of reversible capacity and discharge voltage plateau at the last cycle. It indicates that the OMBB electrolyte is one of the most stable liquid electrolytes in the state-of-the-art Mg/S batteries, which is compatible with S cathode and Mg anode. Cell utilizing OMBB shows a high S utilization of 60.8% (discharge capacity of 1019 mAh g^{-1}) after 100 cycles without obvious capacity fade.[36] The electrochemical performance of this electrolyte reported in literature[36] is referenced to calculate the energy density in a realistic cell system discussed in the following part. Moreover, the mass ratio of S/carbon nanotubes (CNTs)/super-P/PVDF of 64/16/10/10[36] is adopted as the cathode composition, which is reported in the same literature using the OMBB electrolyte. The CNT can disperse super-P to retaining high contact surface area with S and enhance the whole electronic conductivity of cathode composite. We assume that porosity in cathode is 60 vol% to accommodate the volume change of cathode given that cathode porosity should be optimized at 50 to 60 vol% in liquid Li/S cells to achieve a highest energy density.[106] There exists a critical electrolyte volume (ie, critical ratio of E/S has been saved in an Excel S2 [SI]) where liquid electrolyte fills all the pores of cathode and separator exactly. The cathode is coated on a carbon-coated Al foil with a thickness of 18 μm. The reasons why carbon-coated Al foil is used as cathode current collector instead of Cu foil are as follows: (1) Cu current collector could react with S to form copper sulfides,[36,107,108] while carbon-coated Al foil is compatible with S; (2) electrochemical oxidation stability of 0.5 M OMBB electrolyte is 3 V vs Mg/Mg^{2+} measured by linear sweep voltammograms, which indicates a relatively high oxidation stability of electrolyte on Al foil; (3) carbon-coated on two sides of Al foil can protect the Al foil from corrosion of Cl^- in the electrolyte; and (4) the carbon on Al foil can improve adhesion to electrode material, thus achieving a higher S loading. The separator is Celgard 2500 with a thickness of 25 μm. Celgard separator is thinner than glass fiber separator. Therefore, adapting Celgard separator can improve the gravimetric and volumetric energy density of Mg/S batteries. Here, Celgard 2500 is used as a typical Celgard separator in the Mg/S cell (Figure 2A). The porosity of Celgard 2500 is 55 vol%. The cathode and anode tabs are Nickel foils with a fixed mass of 0.16 g per piece. The volume of tab is very small, thus ignored in our calculation. The practical *Eg* and *Ev* can be calculated by Formulas (5) and (6), respectively[109]

$$E_g = \frac{V m_s \cdot C^* A}{\sum W_i} \tag{5}$$

$$E_v = \frac{V m_s \cdot C^* A}{\sum W_i / \rho_i} \tag{6}$$

where V is the average discharge voltage (V), m_s is the S loading (g cm^{-2}) on cathode, C is the specific discharge capacity (mAh g^{-1}), A is the cross-sectional area of S cathode (ie, 8×12 cm^2), and $\sum W_i$ and $\sum W_i/\rho_i$ are the total mass and volume of components of the pouch cell, respectively. The density of components (ρ_i) of the pouch cell is listed in Table S2.

Many parameters can affect Mg/S batteries energy density, such as S loading, S content, S utilization, average discharge voltage, and E/S. First, an ideal cell of 100 wt% S content cathode with a theoretical discharge capacity of 1672 mAh g^{-1} and a theoretical discharge voltage of 1.77 V is analyzed. The S loading and E/S ratio are variables to investigate their effect on battery energy density. The ideal cell's parameters are summarized in Table S3. Based on S loading (m_s), E/S ratio, and cell structure, the mass of each component is calculated in Table S4. Combined with the density of each component, the thickness of each component is calculated in Table S5. Consequently, the *Eg* and *Ev* of ideal pouch cell vs S loading (0-12 mg cm^{-2}) with various E/S ratio (0.5-12 μL mg^{-1}) are plotted in Figure 2B,C, respectively. The energy density generally increases with increasing S loading. For a specified E/S ratio, both the *Eg* and *Ev* increase much faster with S loading less than 6 mg cm^{-2}, and then both tend to increase slowly. For a specified S loading, increasing E/S will decrease energy density rapidly in the range of E/S less than 3 μL mg^{-1}. However, when E/S is further increased, the *Eg* and *Ev* drop slowly.

Considering that practical batteries cannot reach the 100 wt% sulfur content, 100% S utilization and theoretical discharge voltage, we calculated the energy density of a realistic pouch cell. The realistic pouch cell has the cathode composed of 64 wt% S, 16 wt% CNT, 10 wt% super-P, and 10 wt% PVDF binder, with 0.5 M OMBB. The parameters of the realistic pouch cell are shown in Table S6. First, the effect of S loading and E/S ratio on energy density is analyzed. With this OMBB electrolyte, the reported 60.8% S utilization (1019 mAh g^{-1}) and average discharge voltage of 1.2 V are treated as constants.[36] The mass and thickness of components in a realistic pouch cell are calculated in Tables S7 and S8. The resulting energy density as a function of S loading from 1 to 12 mg cm^{-2} and E/S from 0.5 to 12 μL mg^{-1} is shown in Figure 2D,E. Under

low E/S ratio (smaller than 3 μL mg^{-1}), increasing S loading will increase *Eg* and *Ev* rapidly, while under high E/S ratio (larger than 3 μL mg^{-1}), the *Eg* and *Ev* increase slowly with increased S loading, and tend to be flat earlier with S loading larger than 6 mg cm^{-2}. The gravimetric energy density in Figure 2D is close to 200 Wh kg^{-1}, which is comparable with most of present commercial LIBs, with E/S ratio of 1 μL mg^{-1} and S loading of 12 mg cm^{-2}. The *Ev* of cell with E/S ratio of 0.5 and 1 are the same. This is because the liquid electrolyte has not fully filled the total pore volume of cathode and separator. The maximum volumetric energy density in Figure 2E is 257 Wh L^{-1} with E/S of 0.5 or 1 μL mg^{-1} and S loading of 12 mg cm^{-2}, which is much smaller than 600 Wh L^{-1} of present LIB.[110] This is attributed to low discharge voltage (1.2 V) and S utilization (60.8%) in cathode.

In addition to S loading and E/S, S content and sulfur utilization are also investigated towards the *Eg* and *Ev*. According to analyses above, the S loading is fixed at 6 mg cm^{-2}, and the E/S is optimized as 3 μL mg^{-1}. The average discharge voltage is assumed at theoretical voltage (1.77 V). In this case, S content is varied from 20 to 100 wt%, PVDF binder content is fixed at 10 wt%, and the weight ratio of CNT and super-P is maintained at 16/10 (wt/wt), the same as that in the above realistic pouch cell cathode. S utilization is transferred into discharge capacity (mAh g^{-1}) of S. This cell components' mass and thickness are calculated in Tables S9 and S10. Given the above conditions, *Eg* and *Ev* vs S content and discharge capacity are shown in Figure 2F,G. As can be seen, the *Eg* and *Ev* increase slowly as S content increases. This indicates that it is not efficient to increase the energy density of Mg/S batteries by increasing S content only. Instead, S utilization and S content should be considered together to optimize energy density. Further, the S utilization is a key electrochemical parameter to impact both E_g and E_v. Increasing discharge capacity can remarkably increase both E_g and E_v. If the discharge capacity is 1400 mAh g^{-1}, the *Eg* can reach 200 Wh kg^{-1} of the present commercial LIBs with a sulfur content of 50 wt%. Nevertheless, the current maximum discharge capacity reported is 1384 mAh g^{-1} at first discharge with a discharge voltage of 1.37 V when 18 wt% S content is present in cathode.[35] Combining this result with Figure 2F,G, the E_g and E_v are estimated to be much smaller than 200 Wh kg^{-1} and 600 Wh L^{-1}, respectively. Therefore, improving S utilization and average discharge voltage is urgent to improve both *Eg* and *Ev* of Mg/S batteries.

As described, the present Mg/S pouch cell with liquid electrolyte can hardly achieve the *Eg* of 200 Wh kg^{-1} and *Ev* of 600 Wh L^{-1} unless the discharge capacity reaches 1400 mAh g^{-1} and average discharge voltage is close to the theoretical voltage of 1.77 V with optimized S loading (6 mg cm^{-2}) and E/S ratio (3 μL mg^{-1}). However, it may be difficult to achieve these parameters in Mg/S batteries. Moreover, the polysulfide could dissolve in liquid electrolyte and reduce the battery discharge capacity and cycle life. Considering these drawbacks, it is natural to think about Mg/S batteries with SSEs. Inspired by Cao et al,[103] the battery is designed as a pouch cell shown in Figure 3A. The pieces of double-sided coated cathode are 8. The SSE and anode have the same number of pieces, that is, 16. The cathode material is coated on carbon-coated Al foil of 18 μm thickness. The cathode has weight ratio of S/PVDF/Super-P/SSE of 50/10/13.3/26.7, which is referred from solid-state Li/S batteries.[111] Besides, the cathode porosity is set at 15 vol% to accommodate the volume change of the cell,[15] which is an optimized value compared with solid-state Li-S batteries in which 15% to 20% porosity of cathode should be retained[111] and commercial LIBs cathode with a porosity of about 30 vol%.[112] The anode is Mg foil with a capacity of 1.2 times of cathode capacity. No anode current collector is used.[113] By reviewing the reported Mg-ion-based SSEs, $Mg(Tf)_2$-$MgAl_2O_4$-PVDF-HFP ceramic polymer composite electrolyte is chosen in this battery design, which has a high conductivity of 4 mS cm^{-1}, potential window of 3.3 V, and transference number of 0.66, the state-of-the-art Mg-ion solid-state conductor.[114] However, we note that this electrolyte has not yet been tested in Mg/S system. An ideal SSE should possess high ionic conductivity and at the same time be compatible with anode and cathode materials.[115,116] In this design, S utilization and average discharge voltage are fixed at 60.8% (1019 mAh g^{-1}) and 1.2 V, respectively, to be consistent with the realistic liquid Mg/S batteries. The S loading and thickness of SSEs are treated as variables to estimate the *Eg* and *Ev* of this solid-state battery. The above design parameters of this solid-state Mg/S battery are listed in Table S11. The mass and thickness of each component in the solid-state Mg/S pouch cell are calculated in Tables S12 and S13, respectively.

The *Eg* and *Ev* of solid-state Mg/S pouch cell have improved as shown in Figure 3B,C. The cell with thickness of SSE less than 100 μm and S loading more than 7 mg cm^{-2} can all reach 200 Wh kg^{-1} energy density (present energy density of LIBs). Further reducing the thickness of SSE to 10 μm and increase S loading to 12 mg cm^{-2} increase energy density dramatically, reaching 400 Wh kg^{-1} and 700 Wh L^{-1}. Besides, the S loading can affect the *Eg* and *Ev* greatly. The *Eg* and *Ev* increase rapidly with increasing S loading within 4 mg cm^{-2}, while increase rates of the *Eg* and *Ev* become slower when S loading is beyond 4 mg cm^{-2}. However, when the thickness of SSE is larger than 200 μm, the

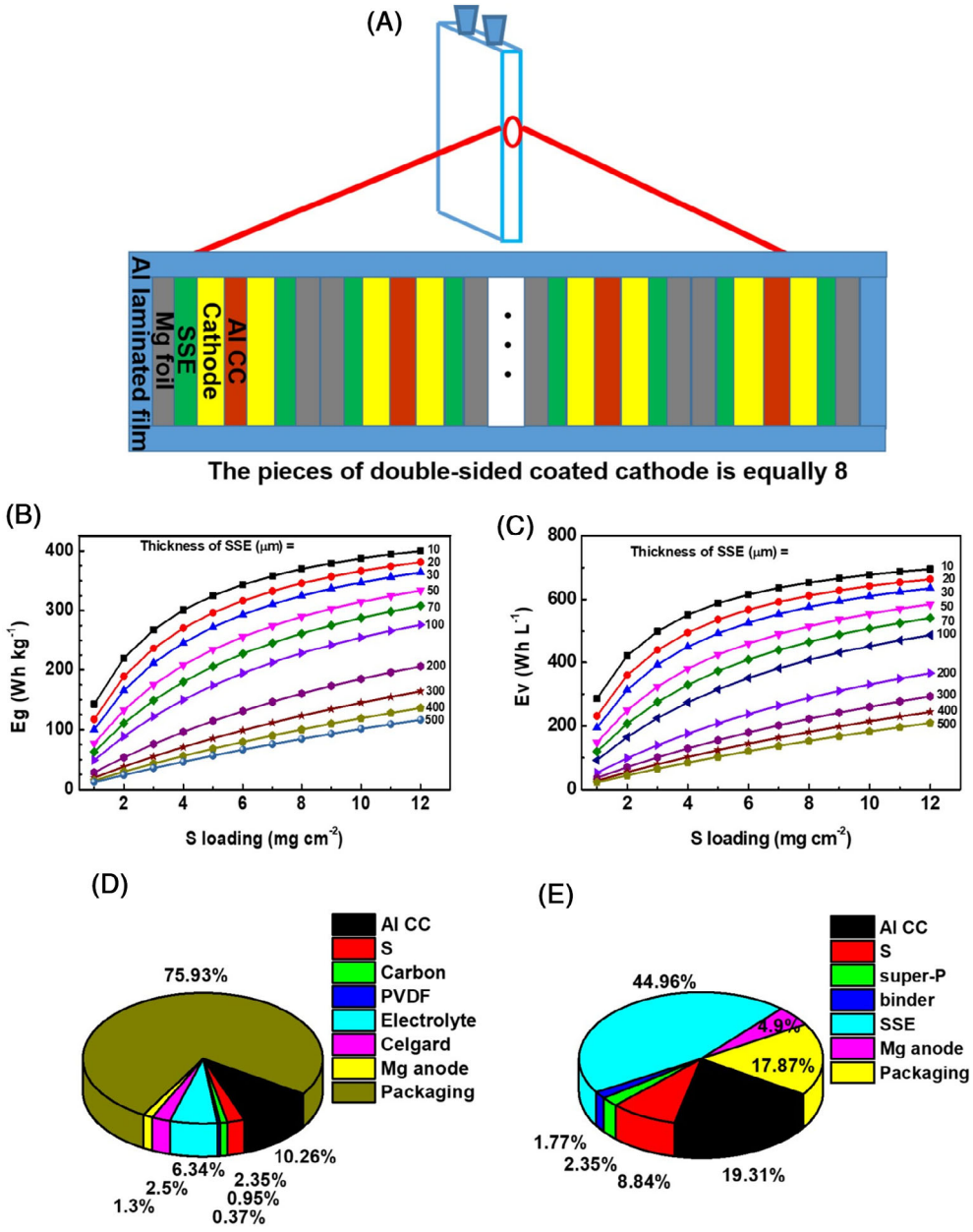

FIGURE 3 Gravimetric and volumetric energy density estimation of magnesium-sulfur (Mg/S) batteries with solid-state electrolytes: A, the structure of pouch cell with solid-state electrolytes; B, the gravimetric; and C, volumetric energy density of solid-state Mg/S pouch cells with varied S loading and thickness of solid-state electrolytes, but fixed average discharge voltage of 1.2 V and S utilization of 60.8% (ie, 1019 mAh g^{-1}); D, mass distribution of pouch cell with liquid electrolyte; and E, solid-state electrolyte with same discharge capacity of 1019 mAh g^{-1} and discharge voltage of 1.2 V. The S loadings in (D) and (E) are same (1 mg cm^{-2}). The E/S in (D) is 2.7 μL mg^{-1} in order to attain 15 vol% porosity in cathode the same as that of cathode in solid-state cell. The thickness of solid-state electrolyte (SSE) separator is 25 μm the same as Celgard 2500

energy density has almost a linear relationship with S loading. The high *Eg* of solid-state Mg/S batteries results from stacked anode and cathode in the solid-state pouch cell, which prominently augments discharge capacity in cell level. Moreover, in the pouch cell with liquid electrolyte, the packaging (containing Al laminated film and tabs) takes up a large percentage of total cell mass (75.93%), while in the solid-state pouch cell the packaging mass percentage (17.87%) decreases and active material mass percentage increases, which contributes to larger gravimetric energy density. This can be proved by cell mass distribution pie figures of the pouch cell with liquid electrolyte (Figure 3D) and SSE (Figure 3E). The average discharge voltage and capacity reported are low (1.2 V and 1019 mAh g^{-1}, respectively), energy density of solid-state Mg/S cell can be further improved when the voltage is raised from 1.2 V to near 1.77 V and discharge capacity is increased from current 1019 to 1672 mAh g^{-1}.

3.2 | Parameterization of Mg/S batteries components based on cost

The cell material cost is calculated based on each material cost and cell structure parameters. The cell structure is consistent with the ones discussed above with liquid electrolyte or SSE. First, the Mg/S pouch cell with liquid electrolyte is considered, which is composed of Mg foil anode, Celgard 2500, S/CNT/Super-P/PVDF cathode, carbon-coated Al foil current collector, and packaging

materials. The price of each material is collected from online data or recent literatures,[117] which is listed in Table S14. The cell material cost is calculated according to Equation (7).[109]

$$P_T = \frac{\sum C_i m_i * A + \sum C_j * A}{V \cdot m_s \cdot C * A} \quad (7)$$

where P_T is the total cost per kWh of the pouch cell, C_i and C_j are cost per gram of material "i" (\$ g^{-1}) and cost per area of component "j" (\$ cm^{-2}), m_i is the mass loading of material "i" (g cm^{-2}), V is the discharge voltage of the cell, m_s is the mass loading of sulfur (g cm^{-2}), C is the discharge capacity (mAh g^{-1}), and A is the material corresponding area. Because there is no commercialized Mg/S cell as a reference, the processing cost is not considered.

The S loading and cost of liquid electrolyte are used as variables to investigate their effect on cell material cost with fixed average discharge voltage of 1.2 V, S utilization of 60.8% (1019 mAh g^{-1}), E/S ratio of 3 μL mg^{-1}. The cell structure is the same as Figure 2A. The cost of 0.5 M OMBB liquid electrolyte used in this cell is calculated to be 23 \$ g^{-1} according to its composition (in SI below Table S16), which is three orders of magnitude higher than liquid electrolyte cost of LIBs.[109] Therefore, the cost of liquid electrolyte is in the range of 0.1 to 23 \$ g^{-1}. The cost of each component of Mg/S batteries is calculated in Table S15. The S loading is transferred into Eg (Wh kg^{-1}) shown in Figure 4A. The cell material cost of the Mg/S pouch cell with liquid electrolyte is much higher compared with the price of LIBs of 174 \$ kWh^{-1} in 2018. The S loading in the range of 1 to 12 mg cm^{-2} has a feeble influence on cell material cost (\$ kWh^{-1}), while the cost of liquid electrolyte has a prominent effect on cell material cost. This indicates that decreasing cost of liquid electrolyte can largely reduce the total price of cell.

Second, the effect of S loading and cost of SSE on cell material cost of solid-state Mg/S cell is considered. The cell structure is the same as shown in Figure 3A. If S loading is aimed at 2 mg cm^{-2} (the reported maximum S loading on Mg/S batteries is 2 mg cm^{-2}), only pouch cell with 10 μm thickness can achieve 200 Wh kg^{-1} under the condition that the discharge capacity of 1019 mAh g^{-1} and average discharge voltage of 1.2 V. Therefore, the thickness of SSE is set at 10 μm. The discharge capacity is 1019 mAh g^{-1}, the average discharge voltage is fixed at 1.2 V, and the S loading is varied from 1 to 12 mg cm^{-2}, consistent with above energy density analysis. The cost of the $Mg(Tf)_2$-$MgAl_2O_4$-PVDF-HFP ceramic polymer composite electrolyte is calculated based on its components price (The components price is in Table S14).

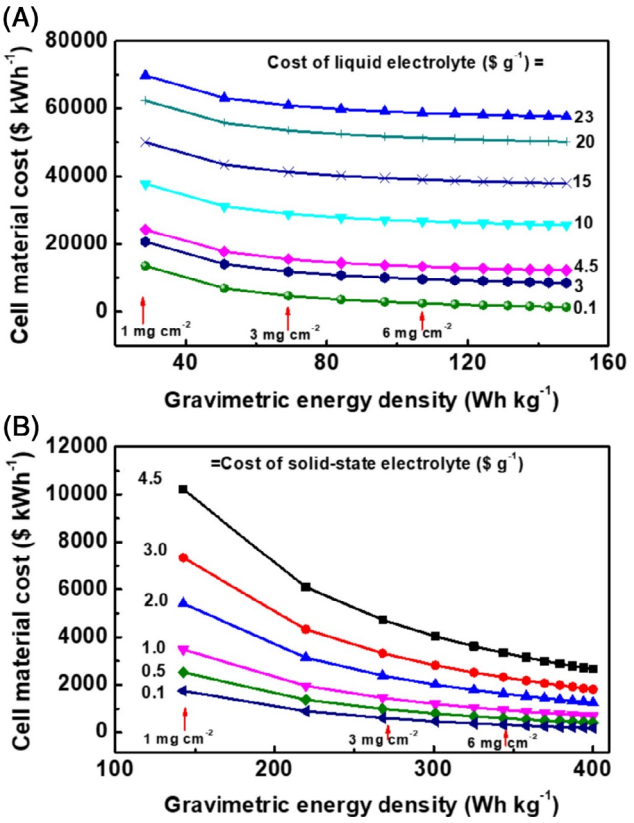

FIGURE 4 The estimated material price for magnesium-sulfur (Mg/S) pouch cells with different liquid electrolyte costs, A, and solid-state electrolyte (SSE) costs, B. The S loading varies from 1 to 12 mg cm^{-2} resulting in different gravimetric energy density and fixed discharge capacity of 1019 mAh g^{-1}, average discharge voltage of 1.2 V in both (A) and (B). In A, the pouch cell has E/S ratio of 3 μL mg^{-1}. In B, the SSE is $Mg(Tf)_2$-$MgAl_2O_4$-PVDF-HFP ceramic polymer composite electrolyte. The 10 μm SSE cost varied from 0.5 to 4.5 \$ g^{-1}

$$C_{SSE} = \frac{C_{EC} + C_{PC} + C_{Mg(Tf)2} + C_{PVDF-HFP} + C_{MgAl2O4}}{m_{solution} + m_{PVDF-HFP} + m_{MgAl2O4}} = 4.5\,\$\,g^{-1}$$

where C and m present cost and mass of each composition, respectively. Based on this calculation, the cost of SSE is assumed to vary from 0.1 to 4.5 \$ g^{-1}. The material cost of solid-state Mg/S batteries is calculated in Table S16. Contrasted to pouch cell with liquid electrolyte, the cell material cost decreases with increased S loading obviously, as shown in Figure 4B. Besides, the cell material cost difference with different cost of SSE is larger in lower S loading (smaller than 2 mg cm^{-2}) than higher S loading (larger than 3 mg cm^{-2}). This indicates that if the energy density of solid-state Mg/S batteries is high, the small fluctuated price of SSE plays a weak function on cell cost. The much cheaper solid-state cell than the cell with liquid electrolyte results from three reasons. First is that SSE price is much smaller than liquid

electrolyte. Second is larger energy density of solid-state pouch cell. The last is that the cost of batteries does not consider the processing cost. This is in stark contrast to the scenario of Li-ion vs solid-state Li battery, where the cost is expected to rise in solid-state batteries.

4 | CONCLUDING REMARKS AND FUTURE PERSPECTIVES

This review comprehensively and critically discusses the Mg/S batteries technology with respect to material development, literature review analysis, energy density, and cost. In spite of recent progress, critical challenges still exist, including the low discharge potential, passivation layer on the Mg anode surface, sluggish ion transfer, the shuttling effect of polysulfides, the relatively low areal capacity, and so forth. Nevertheless, these challenges should be regarded as the driving force for research in the future, which definitely will promote more discoveries of battery materials, battery configurations, and associated battery chemistries.

We propose the following strategies, which might provide deeper insight and pathway to new technologies.

1. The rational design of S hosts as cathode is highly desired to accomplish better performance in Mg/S batteries. Hence, for long life Mg/S batteries, novel conductive hosts need to be designed, which show robust chemical interactions with Mg-PS_x based on interfacial phenomena rather than spatial confinement to mitigate the shuttle effect and possess high electrical conductivity to improve the S utilization. Furthermore, porous nanostructured materials with abundant interfaces and the tenable exposed surfaces may satisfy the possibility of significant enhancement to anchor Mg-PS_x, leading to a stable cyclic performance in Mg/S batteries.
2. Besides the impact of electrolyte on the battery performance, reducing volume and cost of liquid electrolyte in battery are vital to obtain high energy density and low cost Mg/S batteries. Limited by estimated energy density of liquid Mg/S batteries, it is prospective to explore SSEs for much higher energy density.
3. The high capacity alloy anode materials as well as a suitable protective and conductive artificial interphase on Mg anode might be effective approaches to protect the metal surface.
4. Besides the innovations from a material perspective to build better Mg/S batteries, critical mechanistic understanding of Mg/S systems should also deserve special attention.
5. Reasonable parameter design of cell is important to achieve high energy density of Mg/S batteries. For Mg/S batteries with liquid electrolytes, increasing S loading and decreasing E/S ratio are necessary. However, the current reported maximum S loading is 2 mg cm^{-2} and minimum E/S ratio is 64 μL mg^{-1}. Moreover, both reducing cost of liquid electrolyte and improving discharge capacity and voltage are beneficial to obtain the high energy density and low cost for Mg/S batteries. For solid-state Mg/S batteries, it is promising to achieve much higher energy density than liquid Mg/S batteries if a suitable SSE with thickness of several tens of micrometers is prepared.

Mg/S batteries are currently in a nascent stage of progress. With ongoing research progress in lifetime and realistic energy density, a practical and reliable Mg/S cell might be soon realized.

ACKNOWLEDGMENTS

This work was supported by the Oceanic Interdisciplinary Program of Shanghai Jiao Tong University (Grant No. SL2020MS025), NSFC (Grant No. 51801121), Shanghai Commission of Science and Technology (Grant No. 18ZR1421000), and China Scholarship Council.

ORCID

Rameez Razaq https://orcid.org/0000-0002-4107-6744
Yulong Dong https://orcid.org/0000-0001-8352-9361
Shou-Hang Bo https://orcid.org/0000-0001-8963-5261

REFERENCES

1. Choi N-S, Chen Z, Freunberger SA, et al. Challenges facing lithium batteries and electrical double-layer capacitors. *Angew Chem Int Ed*. 2012;5:9994-10024.
2. Goodenough JB, Kim Y. Challenges for rechargeable Li batteries. *Chem Mater*. 2010;22:587-603.
3. Bieker G, Diddens D, Kolek M, et al. Cation-dependent electrochemistry of polysulfides in lithium and magnesium electrolyte solutions. *J Phys Chem C*. 2018;122:21770-21783.
4. Placke T, Kloepsch R, Dühnen S, Winter M. Lithium ion, lithium metal, and alternative rechargeable battery technologies: the odyssey for high energy density. *J Solid State Electrochem*. 2017;21:1939-1964.
5. Janek J, Zeier WG. A solid future for battery development. *Nat Energy*. 2016;1:1-4.
6. Olivetti EA, Ceder G, Gaustad GG, Fu X. Lithium-ion battery supply chain considerations: analysis of potential bottlenecks in critical metals. *Joule*. 2017;1:229-243.
7. McKerracher RD, Ponce de Leon C, Wills RGA, Shah AA, Walsh F. A review of the iron-air secondary battery for energy storage. *Chem Plus Chem*. 2015;80:323-335.
8. Lee J-S, Tai Kim S, Cao R, et al. Metal air batteries with high energy density: Li-air versus Zn-air. *Adv Energy Mater*. 2011;1:34-50.

9. Rahman MA, Wang X, Wen C. High energy density metal-air batteries: a review. *J Electrochem Soc*. 2013;160:A1759-A1771.
10. Wang ZL, Xu D, Xu JJ, Zhang XB. Oxygen electrocatalysts in metal-air batteries: from aqueous to nonaqueous electrolytes. *Chem Soc Rev*. 2014;43:7746-7786.
11. Hardwick LJ, de León CP. Rechargeable multi-valent metal-air batteries. *Johnson Matthey Technol Rev*. 2018;62:134-149.
12. Zhang X, Wang X-G, Xie Z, Zhou Z. Recent progress in rechargeable alkali metal–air batteries. *Green Energy Environ*. 2016;1:4-17.
13. Liu Q, Chang Z, Li Z, Zhang X. Flexible metal-air batteries: progress, challenges, and perspectives. *Small Methods*. 2018;2: 1700231.
14. Xu X, Zhou D, Qin X, et al. A room-temperature sodium-sulfur battery with high capacity and stable cycling performance. *Nat Commun*. 2018;9:3870.
15. Robba A, Vizintin A, Bitenc J, et al. Mechanistic study of magnesium-sulfur batteries. *Chem Mater*. 2017;29:9555-9564.
16. Schmuch R, Wagner R, Hörpel G, Placke T, Winter M. Performance and cost of materials for lithium-based rechargeable automotive batteries. *Nat Energy*. 2018;3:267-278.
17. Berg EJ, Villevieille C, Streich D, Trabesinger S, Novák P. Rechargeable batteries: grasping for the limits of chemistry. *J Electrochem Soc*. 2015;162:A2468-A2475.
18. Bruce PG, Freunberger SA, Hardwick LJ, Tarascon JM. Li-O_2 and Li-S batteries with high energy storage. *Nat Mater*. 2011; 11:19-29.
19. Chung SH, Manthiram A. Current status and future prospects of metal-sulfur batteries. *Adv Mater*. 2019;31:1901125.
20. Hagen M, Hanselmann D, Ahlbrecht K, Maça R, Gerber D, Tübke J. Lithium–sulfur cells: the gap between the state of the art and the requirements for high energy battery cells. *Adv Energy Mater*. 2015;5:1401986.
21. Polyak D. US Geological Survey, Mineral Commodity Summaries; 2018.
22. Zhang Z, Dong S, Cui Z, et al. Rechargeable magnesium batteries using conversiontype cathodes: a perspective and mini-review. *Small Methods*. 2018;2:1905248.
23. Wang P, Buchmeiser MR. Rechargeable magnesium-sulfur battery technology: state of the art and key challenges. *Adv Funct Mater*. 2019;29:1905248.
24. Davidson R, Verma A, Santos D, et al. Formation of magnesium dendrites during electrodeposition. *ACS Energy Lett*. 2018;4:375-376.
25. Yu X, Manthiram A. Performance enhancement and mechanistic studies of magnesium–sulfur cells with an advanced cathode structure. *ACS Energy Lett*. 2016;1:431-437.
26. Kim HS, Arthur TS, Allred GD, et al. Structure and compatibility of a magnesium electrolyte with a sulphur cathode. *Nat Commun*. 2011;2:427.
27. Vinayan BP, Zhao-Karger Z, Diemant T, et al. Performance study of magnesium sulfur battery using a graphene based sulfur composite cathode electrode and a non-nucleophilic Mg electrolyte. *Nanoscale*. 2016;8:3296-3306.
28. Zhao-Karger Z, Zhao X, Wang D, Diemant T, Behm RJ, Fichtner M. Performance improvement of magnesium sulfur batteries with modified non-nucleophilic electrolytes. *Adv Energy Mater*. 2015;5:1401155.
29. Zu C-X, Li H. Thermodynamic analysis on energy densities of batteries. *Energ Environ Sci*. 2011;4:2614-2624.
30. Chen R, Zhao T, Wu F. From a historic review to horizons beyond: lithium-sulphur batteries run on the wheels. *Chem Commun*. 2015;51:18-33.
31. Manthiram A, Fu Y, Chung SH, Zu C, Su YS. Rechargeable lithium–sulfur batteries. *Chem Rev*. 2014;114:11751-11787.
32. Zhao-Karger Z, Fichtner M. Magnesium-sulfur battery: its beginning and recent progress. *MRS Commun*. 2017;7: 770-784.
33. Guo Z, Zhao S, Li T, Su D, Guo S, Wang G. Recent advances in rechargeable magnesium-based batteries for high- efficiency energy storage. *Adv Energy Mater*. 2020;10:1903591.
34. Gao T, Ji X, Hou S, et al. Thermodynamics and kinetics of sulfur cathode during discharge in $MgTFSI_2$-DME electrolyte. *Adv Mater*. 2018;30:1704313.
35. Vinayan BP, Euchner H, Zhao-Karger Z, et al. Insights into the electrochemical processes of rechargeable magnesium–sulfur batteries with a new cathode design. *J Mater Chem A*. 2019;7:25490-25502.
36. Du A, Zhang Z, Qu H, et al. An efficient organic magnesium borate-based electrolyte with non-nucleophilic characteristics for magnesium–sulfur battery. *Energ Environ Sci*. 2017;10:2616-2625.
37. Jackle M, Gross A. Microscopic properties of lithium, sodium, and magnesium battery anode materials related to possible dendrite growth. *J Chem Phys*. 2014;141:174710.
38. Eaves-Rathert J, Moyer K, Zohair M, Pint CL. Kinetic- versus diffusion driven three-dimensional growth in magnesium metal battery anodes. *Joule*. 2020;4:1324-1336.
39. Ding MS, Diemant T, Behm RJ, Passerini S, Giffin GA. Dendrite growth in mg metal cells containing $Mg(TFSI)_2$/glyme electrolytes. *J Electrochem Soc*. 2018;165:A1983-A1990.
40. Jäckle M, Helmbrecht K, Smits M, Stottmeister D, Groß A. Self-diffusion barriers: possible descriptors for dendrite growth in batteries? *Energ Environ Sci*. 2018;11:3400-3407.
41. Bonnick P, Muldoon J. A trip to oz and a peak behind the curtain of magnesium batteries. *Adv Functional Mater*. 2020;30: 1910510.
42. Chen T, Ceder G, Sai Gautam G, Canepa P. Evaluation of Mg compounds as coating materials in mg batteries. *Front Chem*. 2019;7:24.
43. Chu F, Hu J, Tian J, Zhou X, Li Z, Li C. In situ plating of porous mg network layer to reinforce anode dendrite suppression in Li-metal batteries. *ACS Appl Mater Interfaces*. 2018;10: 12678-12689.
44. Yang Y, Wang W, Nuli Y, Yang J, Wang J. Highly active magnesium trifluoromethanesulfonate-based electrolytes for magnesium-sulfur batteries. *ACS Appl Mater Interfaces*. 2019; 11:9062-9072.
45. Salama M, Attias R, Hirsch B, et al. On the feasibility of practical Mg-S batteries: practical limitations associated with metallic magnesium anodes. *ACS Appl Mater Interfaces*. 2018; 10:36910-36917.
46. Ponrouch A, Bitenc J, Dominko R, Lindahl N, Johansson P, Palacin MR. Multivalent rechargeable batteries. *Energy Storage Mater*. 2019;20:253-262.
47. Kong L, Yan C, Huang JQ, et al. A review of advanced energy materials for magnesium-sulfur batteries. *Energy Environ Mater*. 2018;1:100-112.

48. Salama M, Rosy Attias R, Yemini R, Gofer Y, Aurbach D, Noked M. Metal–sulfur batteries: overview and research methods. *ACS Energy Lett*. 2019;4:436-446.
49. Hong X, Mei J, Wen L, et al. Nonlithium metal-sulfur batteries: steps toward a leap. *Adv Mater*. 2019;31:1802822.
50. Zhao-Karger Z, Fichtner M. Beyond intercalation chemistry for rechargeable Mg batteries: a short review and perspective. *Front Chem*. 2018;6:656.
51. Elazari R, Salitra G, Garsuch A, Panchenko A, Aurbach D. Sulfur-impregnated activated carbon fiber cloth as a binder-free cathode for rechargeable Li-S batteries. *Adv Mater*. 2011; 23:5641-5644.
52. Du H, Zhang Z, He J, et al. A delicately designed sulfide graphdiyne compatible cathode for high-performance lithium/magnesium-sulfur batteries. *Small*. 2017;13:1702277.
53. Zhao-Karger Z, Gil Bardaji ME, Fuhr O, Fichtner M. A new class of non-corrosive, highly efficient electrolytes for rechargeable magnesium batteries. *J Mater Chem A*. 2017;5: 10815-10820.
54. Muthuraj D, Ghosh A, Kumar A, Mitra S. Nitrogen and sulfur doped carbon cloth as current collector and polysulfide immobilizer for magnesium-sulfur batteries. *Chem Electro Chem*. 2018;6:684-689.
55. Zhou X, Tian J, Hu J, Li C. High rate magnesium-sulfur battery with improved cyclability based on metal-organic framework derivative carbon host. *Adv Mater*. 2018;30:1704166.
56. Wei S, Xu S, Agrawral A, et al. A stable room-temperature sodium-sulfur battery. *Nat Commun*. 2016;7:11722.
57. Ji X, Lee KT, Nazar LF. A highly ordered nanostructured carbon-sulphur cathode for lithium-sulphur batteries. *Nat Mater*. 2009;8:500-506.
58. Zheng G, Yang Y, Cha JJ, Hong SS, Cui Y. Hollow carbon nanofiber encapsulated sulfur cathodes for high specific capacity rechargeable lithium batteries. *Nano Lett*. 2011;11: 4462-4467.
59. Gao T, Hou S, Wang F, et al. Reversible S0/MgSx redox chemistry in a MgTFSI2 /MgCl2/DME electrolyte for rechargeable Mg/S batteries. *Angew Chem Int Ed*. 2017;56:13526-13530.
60. Zhang BW, Sheng T, Liu YD, et al. Atomic cobalt as an efficient electrocatalyst in sulfur cathodes for superior room-temperature sodium-sulfur batteries. *NatCommun*. 2018;9: 4082.
61. Zhang BW, Sheng T, Wang Y, et al. Long-life room-temperature sodium-sulfur batteries by virtue of transition-metal nanocluster-sulfur interactions. *Angew Chem Int Ed*. 2019;58:1484-1488.
62. Jeong T-G, Choi DS, Song H, et al. Heterogeneous catalysis for lithium–sulfur batteries: enhanced rate performance by promoting polysulfide fragmentations. *ACS Energy Lett*. 2017; 2:327-333.
63. Lin H, Yang L, Jiang X, et al. Electrocatalysis of polysulfide conversion by sulfur-deficient MoS_2 nanoflakes for lithium–sulfur batteries. *Energ Environ Sci*. 2017;10:1476-1486.
64. Lim WG, Kim S, Jo C, Lee J. A comprehensive review of materials with catalytic effects in Li-S batteries: enhanced redox kinetics. *Angew Chem Int Ed*. 2019;58:18746-18757.
65. Razaq R, Zhang N, Xin Y, Li Q, Wang J, Zhang Z. Electrocatalytic conversion of lithium polysulfides by highly dispersed ultrafine Mo_2C nanoparticles on hollow N-doped carbon flowers for Li-S batteries. *EcoMat*. 2020;2:e12020.
66. Doe RE, Han R, Hwang J, et al. Novel, electrolyte solutions comprising fully inorganic salts with high anodic stability for rechargeable magnesium batteries. *Chem Commun*. 2014;50: 243-245.
67. Muldoon J, Bucur CB, Oliver AG, et al. Electrolyte roadblocks to a magnesium rechargeable battery. *Energ Environ Sci*. 2012; 5:5941-5950.
68. Tutusaus O, Mohtadi R. Paving the way towards highly stable and practical electrolytes for rechargeable magnesium batteries. *Chem Electro Chem*. 2015;2:51-57.
69. Xu Y, Zhou G, Zhao S, et al. Improving a Mg/S battery with YCl_3 additive and magnesium polysulfide. *Adv Sci*. 2019;6: 1800981.
70. Zhao X, Yang Y, NuLi Y, Li D, Wang Y, Xiang X. A new class of electrolytes based on magnesium bis(diisopropyl)amide for magnesium-sulfur batteries. *Chem Commun*. 2019;55:6086-6089.
71. Liu T, Shao Y, Li G, et al. A facile approach using $MgCl_2$ to formulate high performance Mg^{2+} electrolytes for rechargeable Mg batteries. *J Mater Chem A*. 2014;2:3430-3438.
72. Bian P, NuLi Y, Abudoureyimu Z, Yang J, Wang J. A novel thiolate-based electrolyte system for rechargeable magnesium batteries. *Electrochim Acta*. 2014;121:258-263.
73. Gao T, Noked M, Pearse AJ, et al. Enhancing the reversibility of Mg/S battery chemistry through Li^+ mediation. *J Am Chem Soc*. 2015;137:12388-12393.
74. Ha SY, Lee YW, Woo SW, et al. Magnesium(II) bis(-trifluoromethane sulfonyl) imide based electrolytes with wide electrochemical windows for rechargeable magnesium batteries. *ACS Appl Mater Interfaces*. 2014;6:4063-4073.
75. Li W, Cheng S, Wang J, et al. Synthesis, crystal structure, and electrochemical properties of a simple magnesium electrolyte for magnesium/sulfur batteries. *Angew Chem Int Ed*. 2016;55: 6406-6410.
76. Zhang Z, Cui Z, Qiao L, et al. Novel design concepts of efficient mg-ion electrolytes toward high-performance magnesium-selenium and magnesium-sulfur batteries. *Adv Energy Mater*. 2017;7:1602055.
77. Zhang Y, Xie J, Han Y, Li C. Dual-salt mg-based batteries with conversion cathodes. *Adv Funct Mater*. 2015;25:7300-7308.
78. Tian J, Cao D, Zhou X, Hu J, Huang M, Li C. High-capacity Mg-organic batteries based on nanostructured rhodizonate salts activated by Mg-Li dual-salt electrolyte. *ACS Nano*. 2018; 12:3424-3435.
79. Jaschin PW, Gao Y, Li Y, Bo S-H. A materials perspective on magnesium-ion-based solid-state electrolytes. *J Mater Chem A*. 2020;8:2875-2897.
80. Tao X, Liu Y, Liu W, et al. Solid-state lithium-sulfur batteries operated at 37°C with composites of nanostructured $Li_7La_3Zr_2O_{12}$/carbon foam and polymer. *Nano Lett*. 2017;17: 2967-2972.
81. Yu X, Manthiram A. Sodium-sulfur batteries with a polymer-coated NASICON-type sodium-ion solid electrolyte. *Matter*. 2019;1:439-451.
82. Anuar NK, Mohamed NS. Structural and electrical properties of novel $Mg_{0.9+0.5y}Zn_{0.4}Al_yZr_{1.6-y}(PO_4)_3$ ceramic electrolytes

synthesized via nitrate sol-gel method. *J Sol-Gel Sci Technol*. 2016;80:249-258.
83. Canepa P, Bo S-H, Gautam GS, et al. High magnesium mobility in ternary spinel chalcogenides. *Nat Commun*. 2017;8:1359.
84. Miner EM, Park SS, Dinca M, et al. High Li^+ and Mg^{2+} conductivity in a Cu-azolate metal-organic framework. *J Am Chem Soc*. 2019;141:4422-4427.
85. Muldoon J, Bucur CB, Gregory T, et al. Quest for nonaqueous multivalent secondary batteries: magnesium and beyond. *Chem Rev*. 2014;114:11683-11720.
86. Zhao-Karger Z, Liu R, Dai W, et al. Toward highly reversible magnesium–sulfur batteries with efficient and practical Mg[B(hfip)4]2 electrolyte. *ACS Energy Lett*. 2018;3:2005-2013.
87. He P, Ford HO, Merrill LC, Schaefer JL. Investigation of the effects of copper nanoparticles on magnesium–sulfur battery performance: how practical is metallic copper addition? *ACS ApplEnergy Mater*. 2019;2:6800-6807.
88. Higashi S, Miwa K, Aoki M, Takechi K. A novel inorganic solid state ion conductor for rechargeable Mg batteries. *Chem Commun*. 2014;50:1320-1322.
89. Hu XC, Shi Y, Lang SY, et al. Direct insights into the electrochemical processes at anode/electrolyte interfaces in magnesium-sulfur batteries. *Nano Energy*. 2018;49:453-459.
90. Mohtadi R, Mizuno F. Magnesium batteries: current state of the art, issues and future perspectives. *Beilstein J Nanotechnol*. 2014;5:1291-1311.
91. Yoo HD, Shterenberg I, Gofer Y, Gershinsky G, Pour N, Aurbach D. Mg rechargeable batteries: an on-going challenge. *Energ Environ Sci*. 2013;6:2265-2279.
92. Aurbach D, Weissman I, Gofer Y, Levi E. Nonaqueous magnesium electrochemistry and its application in secondary batteries. *Chem Rec*. 2003;3:61-73.
93. Sievert B, Hacker J, Bienen F, Wagner N, Friedrich KA. Magnesium sulfur battery with a new magnesium powder anode. *ECS Trans*. 2017;77:413-424.
94. Liu Z, Lee J, Xiang G, et al. Insights into the electrochemical performances of Bi anodes for Mg ion batteries using 25Mg solid state NMR spectroscopy. *Chem Commun*. 2017;53:743-746.
95. Ding C, Huang L, Guo Y, et al. An ultra-durable gel electrolyte stabilizing ion deposition and trapping polysulfides for lithium-sulfur batteries. *Energy Storage Mater*. 2020;27:25-34.
96. Cha E, Patel MD, Park J, et al. 2D MoS_2 as an efficient protective layer for lithium metal anodes in high-performance Li-S batteries. *Nat Nanotechnol*. 2018;13:337-344.
97. Lv R, Guan X, Zhang J, Xia Y, Luo J. Enabling Mg metal anodes rechargeable in conventional electrolytes by fast ionic transport interphase. *Natl Sci Rev*. 2020;7:333-341.
98. Aurbach D, Gizbar H, Schechter A, et al. Electrolyte solutions for rechargeable magnesium batteries based on organomagnesium chloroaluminate complexes. *J Electrochem Soc*. 2002;149:A115-A121.
99. Zhang J, Guan X, Lv R, Wang D, Liu P, Luo J. Rechargeable Mg metal batteries enabled by a protection layer formed in vivo. *Energy Storage Mater*. 2020;26:408-413.
100. Canepa P, Gautam GS, Malik R, et al. Understanding the initial stages of reversible mg deposition and stripping in inorganic nonaqueous electrolytes. *Chem Mater*. 2015;27:3317-3325.
101. Canepa P, Jayaraman S, Cheng L, et al. Elucidating the structure of the magnesium aluminum chloride complex electrolyte for magnesium-ion batteries. *Energ Environ Sci*. 2015;8:3718-3730.
102. Xu Y, Ye Y, Zhao S, et al. *In situ* X-ray absorption spectroscopic investigation of the capacity degradation mechanism in Mg/S batteries. *Nano Lett*. 2019;19:2928-2934.
103. Cao W, Zhang J, Li H. Batteries with high theoretical energy densities. *Energy Storage Mater*. 2020;26:46-55.
104. Haynes WM. *CRC Handbook of Chemistry and Physics*. Boca Raton, London: CRC Press; 2014.
105. Cui C, Yang C, Eidson N, Chen J, et al. A highly reversible, dendrite-free lithium metal anode enabled by a lithium-fluoride-enriched interphase. *Adv Mater*. 2020;32:1906427.
106. Kang N, Lin Y, Yang L, et al. Cathode porosity is a missing key parameter to optimize lithium-sulfur battery energy density. *NatCommun*. 2019;10:4597.
107. Du A, Zhao Y, Zhang Z, et al. Selenium sulfide cathode with copper foam interlayer for promising magnesium electrochemistry. *Energy Storage Mater*. 2020;26:23-31.
108. Lee B, Choi J, Na S, et al. Critical role of elemental copper for enhancing conversion kinetics of sulphur cathodes in rechargeable magnesium batteries. *Appl Surf Sci*. 2019;484:933-940.
109. McCloskey BD. Attainable gravimetric and volumetric energy density of Li-S and li ion battery cells with solid separator-protected Li metal anodes. *J Phys Chem Lett*. 2015;6:4581-4588.
110. Mo R, Tan X, Li F, et al. Tin-graphene tubes as anodes for lithium-ion batteries with high volumetric and gravimetric energy densities. *Nat Commun*. 2020;11:1374.
111. Yang X, Luo J, Sun X. Towards high-performance solid-state Li–S batteries from fundamental understanding to engineering design. *Chem Soc Rev*. 2020;49:2140-2195.
112. Betz J, Bieker G, Meister P, Placke T, Winter M, Schmuch R. Theoretical versus practical energy: a plea for more transparency in the energy calculation of different rechargeable battery systems. *Adv Energy Mater*. 2019;9:1803170.
113. Liu L, Ren D, Liu F, et al. A review of dissimilar welding techniques for magnesium alloys to aluminum alloys. *Materials*. 2014;7:3735-3757.
114. Sharma J, Hashmi S. Magnesium ion-conducting gel polymer electrolyte nanocomposites: effect of active and passive nanofillers. *Polym Compos*. 2018;40:1295-1306.
115. Tian Y, Shi T, Richards WD, et al. Compatibility issues between electrodes and electrolytes in solid-state batteries. *Energ Environ Sci*. 2017;10:1150-1166.
116. Xiao Y, Wang Y, Bo S-H, et al. Understanding interface stability in solid-state batteries. *Nat Rev Mater*. 2019;5:105-126.
117. Yoo HD, Jokisaari JR, Yu Y-S, et al. Intercalation of magnesium into a layered vanadium oxide with high capacity. *ACS Energy Lett*. 2019;4:1528-1534.

AUTHOR BIOGRAPHIES

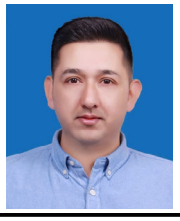

Rameez Razaq received his MPhil degree in Physical Chemistry from University of Peshawar, Pakistan. In 2019, he completed his PhD degree in Chemical Engineering and Technology from the University of Jinan,

China. Then, he joined Dr S.-H. B.'s group as a postdoctoral fellow at the University of Michigan Shanghai Jiao Tong University Joint Institute, China. His current research focuses on the solid-state electrolytes for Magnesium-sulfur batteries.

PING LI received her bachelor degree in Material Science and Engineering School in Huazhong University of Science and Technology, China. Now she is pursuing her PhD degree in University of Michigan-Shanghai Jiao Tong University Joint Institute, China. Her current research focuses on rechargeable Magnesium-sulfur batteries and material failure in battery.

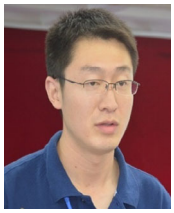

Dr **YAO LI** received his PhD degree in Material Science from the Shanghai Jiao Tong University, China in 2015. He joined as a research associate at Shanghai Jiao Tong University at 2015. He has a visiting scholar program at Massachusetts institute of technology at 2020. He is working on research of bioinspired material and carbon material, as well as their application on energy conversion, storage and environment treatment.

YA MAO is a senior engineer in State Key Laboratory of Space Power-Sources Technology, Shanghai Institute of Space Power-Sources. She received her PhD degree in 2013 from Institute of Physics, University of Chinese Academy of Sciences. Her research is focused on energy storage device, such as lithium ion batteries, and advanced high energy density secondary batteries with multielectron reaction.

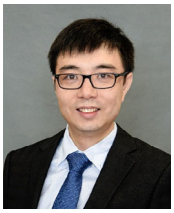

DR SHOU-HANG BO received his BS degree in Chemistry from Fudan University in 2009 and his PhD degree in Chemistry from Stony Brook University in 2014. Since 2014, Dr S.-H. B. has been a postdoctoral fellow at the Department of Materials Science and Engineering, Massachusetts Institute of Technology, and Materials Sciences Division, Lawrence Berkeley National Laboratory. Dr Bo joined the University of Michigan-Shanghai Jiao Tong University Joint Institute in 2017 as a tenure-track assistant professor. His recent research interests include fast ionic conductors for use in solid-state batteries, optimization of the chemical and mechanical properties of solid-state interfaces in batteries, and imaging of solid-state batteries.

SUPPORTING INFORMATION

Additional supporting information may be found online in the Supporting Information section at the end of this article.

How to cite this article: Razaq R, Li P, Dong Y, Li Y, Mao Y, Bo S-H. Practical energy densities, cost, and technical challenges for magnesium-sulfur batteries. *EcoMat*. 2020;2:e12056. https://doi.org/10.1002/eom2.12056